

Combined Analysis of DNA Ploidy, Proliferation, and Apoptosis in Paraffin-Embedded Cell Material by Flow Cytometry

Thomas Heiden, Esmeralda Castañón-Vélez, Leif C. Andersson, and Peter Biberfeld

Immunopathology Laboratory (TH, EC-V, LCA, PB), Cancer Center Karolinska, Karolinska Institute, Stockholm, Sweden; and Department of Pathology (LCA), Haartman Institute, University of Helsinki, Finland

SUMMARY: A flow cytometric assay was developed for correlated measurement of DNA content and apoptotic DNA strand breaks in cell nuclei of formalin-fixed, paraffin-embedded tissues. The assay allows a combined analysis of cell ploidy, proliferation, and apoptosis in sections of fixed paraffin-embedded archival or fresh tissue/cell specimens. It is based on (a) proteolytic release of cell nuclei from deparaffinized and rehydrated 90- μm thick sections of the fixed embedded specimen, (b) the inactivation of the protease, (c) FITC-labeling of DNA strand breaks by the terminal deoxynucleotidyl transferase (TdT)-mediated FITC-dUTP nick end-labeling (TUNEL) reaction, and (d) DNA staining with 4'6-diamidino-2-phenyleindole. The fluorescence was recorded with a double-beam flow cytometer equipped with a mercury arc lamp and an argon ion laser. Cytograms obtained with this assay correlated closely with those produced using nonembedded material from the same specimen. Furthermore, a significant correlation was found between flow cytometric analysis of apoptosis in cell nuclei released from paraffin blocks and conventional evaluation of TUNEL on (corresponding) sections ($p < 0.001$). Since necrotic cells can stain positively by TUNEL, the possibility to microscopically select nonnecrotic tumor regions for flow cytometric analysis is an important advantage of the assay. (*Lab Invest* 2000, 80:1207-1213).

It is now well established that cell proliferation and/or apoptotic cell death are abnormally regulated in most tumors. Thus, an imbalance between cell gain by mitotic cell divisions and cell loss by apoptosis is regarded as a central element in tumor growth (Fisher, 1994). However, in contrast to studies on cell proliferation, only a few quantitative studies (Baretton et al, 1996; Czader et al, 1996; Dowsett et al, 1996, 1998; Ellis et al, 1996, 1997; Lipponen et al, 1994; Samoszuk et al 1996) have related apoptosis in human malignancies to other pathologic or clinical data. One requirement for statistical confidence when estimating small fractions of cells, like apoptotic cells in tumors, is to score large numbers of cells. This can be achieved by flow cytometry (FCM). Cells in an advanced stage of apoptosis with degradation of DNA can be labeled with the terminal deoxynucleotidyl transferase (TdT)-mediated FITC-dUTP nick end labeling (TUNEL) assay (Gavrieli et al, 1992), which, combined with FCM, allows the detection of even rare apoptotic events in suspended cell populations (Listman et al, 1998; Olano et al, 1996). Furthermore, such cell preparations make possible a combination of the evaluation of apoptosis, ploidy, and proliferation in the same cell population (Gorczyca et al, 1993). This

approach has been applied to the analysis of fresh tumor cell preparations sampled by fine-needle aspiration (Dowsett et al, 1998; Gorczyca et al, 1994). If a necrotic tissue is included in such specimens, a marked increase in TUNEL-positive events can occur and disturb the specific evaluation of apoptotic cells (Dowsett et al, 1998). In the present study, we have therefore considered the possibility of using thick sections of nonnecrotic, paraffin-embedded tissues morphologically selected by microscopy for proteolytic enucleation (Hedley et al, 1983; Heiden et al, 1991) and DNA content/TUNEL analysis with FCM. Using FCM, we have compared ploidy, proliferation, and apoptosis in the nuclei of such enucleated sections with the nuclei of corresponding nonembedded specimens, as well as whole-cell preparations and conventional microscopic analysis of apoptosis by the TUNEL reaction on sections.

Results

Comparison of Cell Nuclei from Paraffin-Embedded and Nonembedded Specimens

The microscopic appearance of cell nuclei released from one paraffin section (90 μm) of a tonsil after FITC-labeling by TUNEL and staining with 4'6-diamidino-2-phenyleindole (DAPI) is shown in Figure 1. Most nuclei show a weak background of FITC-fluorescence, but a fraction (~5%) of nuclei is strongly FITC-labeled, whereas TdT-negative controls did not contain such strongly labeled nuclei. Comparison of

Received February 15, 2000.

Supported by the Karolinska Institute and the Swedish Cancer Society.

Address reprint requests to: Dr. Thomas Heiden, Immunopathology Laboratory, Karolinska Institute/Hospital, CCK, R8, S-17176 Stockholm, Sweden. Fax: 46 8 51775042; E-mail: Thomas.Heiden@onkpat.ki.se

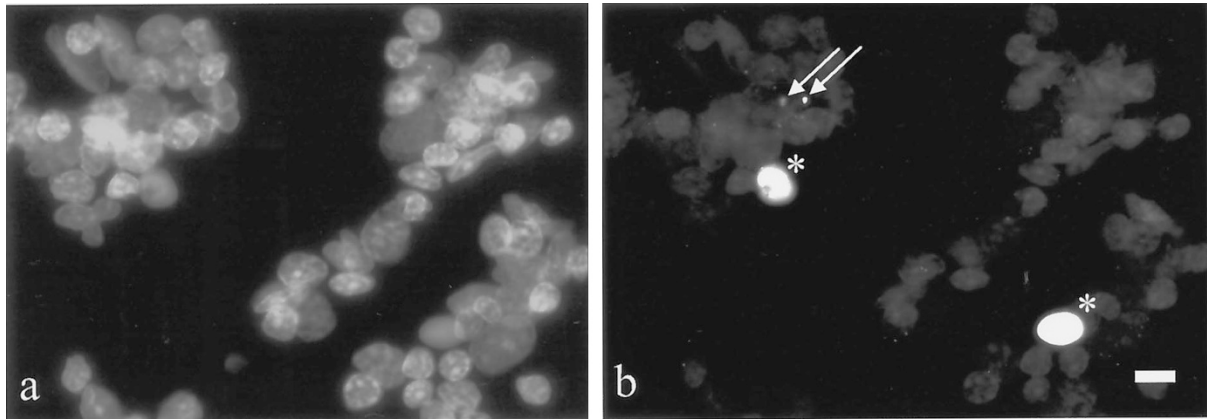


Figure 1.

Fluorescence micrographs of cell nuclei released from one section of a paraffin-embedded tonsil, prepared as described in the “Materials and Methods” section: (a) 4',6-diamidino-2-phenylindole (DAPI) and (b) TdT-mediated FITC-dUTP nick end-labeling (TUNEL)-FITC. A distinct discrimination between TUNEL-negative cell nuclei and TUNEL-positive apoptotic nuclei (*) and chromatin bodies (arrows) can be seen. Scale bar = 10 μ m.

flow cytograms of cell nuclei from paraffin sections and cell nuclei from matched nonembedded specimens shows quite similar cytogram patterns (Fig. 2, a and b). The paired samples were highly correlated for S-phase (data not shown) and apoptosis ($r > 0.96$) and show, in U937 specimens, an equivalent steep increase of the percentage of apoptotic cell nuclei after 1 hour treatment with tumor necrosis factor α (TNF α) (Fig. 3). Furthermore, similar coefficient of variation (CV) values for the DAPI-DNA analysis were found. Thus, the mean percentage CV values \pm sd of

G1 events were 3.7 ± 0.9 and 3.4 ± 0.9 for paraffin sections versus nonembedded specimens (paired t test, $P = 0.08$) (Figure 2, a and b).

Comparison of Intact U937 Cells and Cell Nuclei from Paraffin-Embedded U937 Cells

Cytograms of cell nuclei from paraffin-embedded U937 cells compared with cytograms of intact (nondigested) U937 cells had slightly smaller fractions of TUNEL-negative G1 events (mean values, 33.2% vs

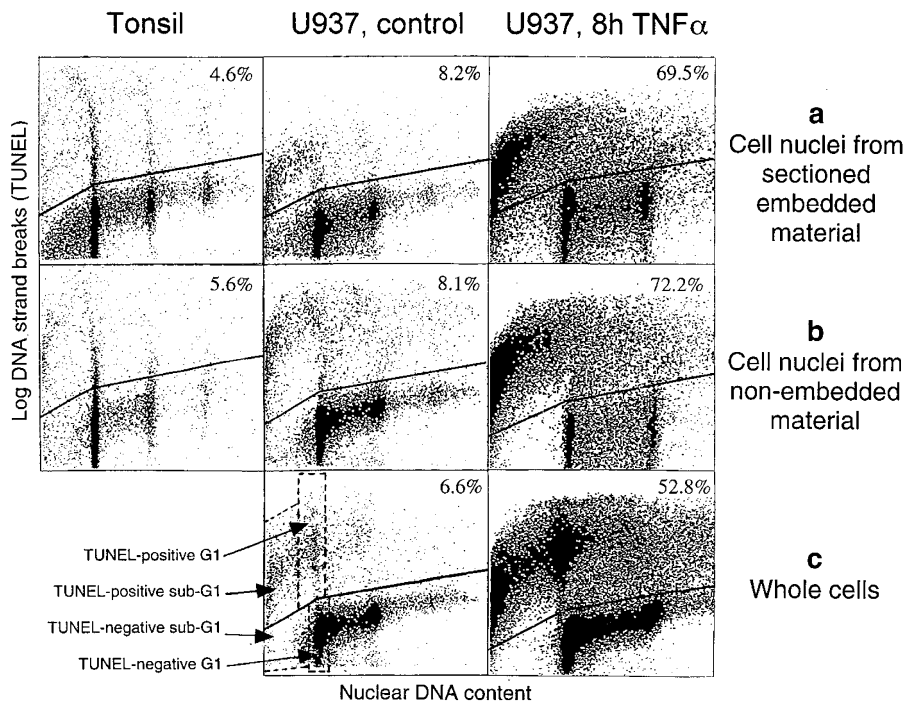


Figure 2.

Comparison of the DNA content and TUNEL analysis in cell nuclei from matched tonsil and U937 cell samples prepared by extraction and staining of cell nuclei from paraffin-embedded (a) and nonembedded material (b) and by staining of whole U937 cells (c). The U937 cells were analyzed before (control) and after triggering of apoptosis (8 hours TNF α). The lines indicate decision boundaries for counting of TUNEL-positive events (solid lines) and sub-G1- and G1-phase events (broken lines). Percentages of TUNEL-positive events are indicated.

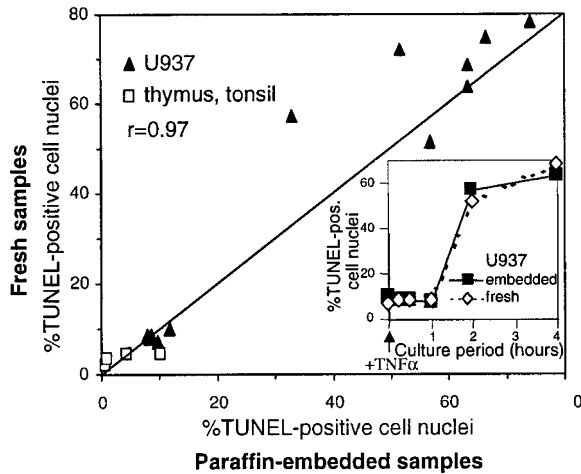


Figure 3.

Comparison of fractions of TUNEL-positive apoptotic cell nuclei in matched samples prepared by extraction and staining of cell nuclei from paraffin-embedded and nonembedded cells. One thymus and three tonsil biopsies and thirteen U937 samples, the latter fixed after different times of exposure to TNF α , were prepared (see "Material and Methods" section) and analyzed by flow cytometry (FCM). The lines of identical values and the coefficient of correlation (*r*) are shown. Inset: Effect of TNF α treatment as determined by counting TUNEL-positive cell nuclei from paraffin-embedded and nonembedded U937 cells.

36.9%) and larger fractions of TUNEL-negative sub-G1 events (4.6% vs 1.1%) (Fig. 2, a and c; Table 1). In the TUNEL-positive region, cytograms of cell nuclei from embedded U937 cells compared with cytograms of whole cells clearly showed fewer G1 events (3.1% vs 10.5%) and unproportionally larger sub-G1 fractions (29.2% vs 13.6%) corresponding to more total TUNEL-positive events (37.1% vs 31.4%) (Fig. 2, a and c; Table 1).

Comparative Flow and Histologic TUNEL Analysis of Paraffin-Embedded Specimens and Reproducibility of FCM Analysis

As illustrated in Figure 4, comparison between TUNEL-positive scores in nonnecrotic regions of the specimens by flow and microscopy showed a statistically significant correlation ($r = 0.96, P < 0.001$), although a tendency to higher values by FCM analysis was apparent (paired *t* test, $P < 0.05$). In two samples (each marked with "x" in Fig. 4), large necrotic areas,

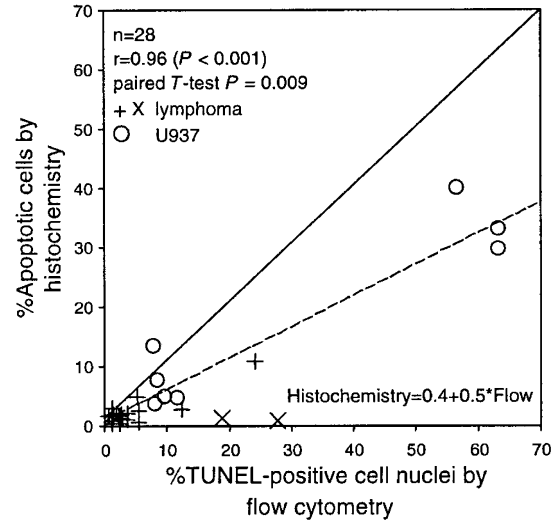


Figure 4.

Comparison between fractions of TUNEL-positive apoptotic cells evaluated by histochemistry and TUNEL-positive events measured by FCM. The analysis was done in adjacent sections of 20 paraffin-embedded lymphoma tissues (10 primary and 10 secondary tumors from inoculated severe combined immunodeficiency mice) and eight U937 specimens. The line of identical values (solid line), the least-squares line (dashed line), and the results of correlation analysis and paired *t* test are shown. Samples with necrotic regions (x) were excluded from correlation analysis and *t* test.

rich in TUNEL-positive nuclei, resulted in a marked increase in TUNEL-positive events in the FCM analysis, disturbing the specific evaluation of apoptotic cells.

The reproducibility of TUNEL staining and analysis by FCM was tested in a fixed-cell suspension of rat thymocytes. In six aliquots of the same suspension, stained with different lots of the reaction kit over a period of 1 year, $24.0\% \pm 1.3\%$ (mean \pm SD) TUNEL-positive G1 cells were found. The reproducibility in individual sections ($n = 8$) from the same paraffin-embedded tonsil was $4.0\% \pm 1.3\%$ for TUNEL-positive fractions and $4.7\% \pm 1.7\%$ for S-phase fractions. Thus, the FCM assay showed a good reproducibility of analysis.

Discussion

Our results indicate that cytometry can be developed for the combined analysis of DNA ploidy, proliferation,

Table 1. Comparison of Fractions of Events in 5 Histogram Regions^a in 13 Paired U937 Samples of Whole Nonembedded Cells and Bare Cell Nuclei Extracted from Sections of Paraffin-Embedded Cells

	Nonembedded whole cells*	Embedded cell nuclei*	Paired <i>t</i> -test <i>P</i>
% TUNEL-negative G1	36.9 \pm 14.9	33.2 \pm 17.5	0.042
% TUNEL-negative sub-G1	1.1 \pm 0.6	4.6 \pm 1.5	<0.001
% TUNEL-positive G1	10.5 \pm 8.6	3.1 \pm 3.6	0.002
% TUNEL-positive sub-G1	13.6 \pm 13.2	29.2 \pm 22.3	0.004
% all TUNEL-positive events	31.4 \pm 24.6	37.1 \pm 28.1	0.041

^a The histogram regions of TUNEL-positive and -negative G1 and sub-G1 events are indicated in Figure 4 with broken lines; the histogram region of all TUNEL-positive events corresponds to the range above the solid line. S- and G2-phase events were not evaluated separately. G1, G1-phase fraction.

* Mean values \pm SD.

and apoptosis in paraffin-embedded cells and tissues. The assay presented here can be used in studies of newly diagnosed as well as archival tumor specimens from patients under treatment or with known outcome of disease, and the results can be related to other clinical or pathologic data. In particular, the flow data can be correlated with histologic findings in adjacent sections allowing microscopic selection of tissues for FCM analysis.

About 70% of solid tumors are aneuploid by FCM (Barlogie et al, 1983), and in such tumors, one can readily discriminate between growth parameters of neoplastic (aneuploid) cells and other tissue elements using the ploidy data in the histogram. To make the best out of FCM data in diploid tumors, one can estimate, with microscopic analysis of adjacent sections, portions of nonneoplastic reactive cells in the tumor regions selected for FCM.

It has been previously reported that necrotic cell nuclei that are not completely disintegrated can also be recorded in the TUNEL-positive fraction by FCM (Dowsett et al, 1998). This was also found to be true in the present study in two samples containing large necrotic areas (Fig. 4). Obviously, the possibility of minimizing contributions from necrotic tissue regions by selecting representative nonnecrotic tumor areas for FCM analysis appears to be an important advantage of the described assay.

The analysis of enucleated sectioned specimens showed good reproducibility and correlated closely with the analysis of matched enucleated nonsectioned samples from tissues and cultured cells (U937) (Fig. 2, a and b, and 3). Comparison of the analysis of enucleated sectioned specimens with nonenucleated whole cells (U937) showed that cytograms of cell nuclei from sections had slightly smaller fractions of TUNEL-negative G1 and larger fractions of TUNEL-negative sub-G1 events (Fig. 2, a and c; Table 1), which obviously is caused by an increase in nuclear fragments from sectioned cells. A much stronger decrease of TUNEL-positive G1 events and increase of TUNEL-positive sub-G1 events was visible in the enucleated sectioned samples compared with specimens with whole cells. This probably reflects a release of chromatin bodies from G1 cells in advanced apoptosis by the enucleation procedure (Fig. 1), which are measured individually by FCM. Accordingly, the total fraction of TUNEL-positive events was lower in the samples of whole cells analyzed by FCM (Table 1) or counted in the sections (Fig. 4) than in the samples of enucleated sectioned specimens. However, results obtained from standardized evaluation of nuclear samples can be directly related to each other, and when compared with results obtained in whole cells, the bias could be corrected by compensating with a definite factor as shown in Figure 4.

The background levels of the TUNEL staining appeared to increase with stronger protease treatment and aggregation of autofluorescent erythrocytes with TUNEL-negative cell nuclei (data not shown). These problems were avoided by monitoring and stopping the protease treatment as soon as the nuclei appeared

released of cytoplasm and by using Tris buffer instead of ethanol to remove the formaldehyde after inactivation of the protease. Long fixation delay (> 24 hours, room temperature) also increased considerably the background levels in all cells (data not shown). Thus, proper control of the preparation with microscopic checks ensures that no false-positive TUNEL results are obtained.

In this study, a double beam flow cytometer equipped with a mercury arc lamp and an argon ion laser was used for a highly specific and sensitive measurement of DAPI and FITC. The described optics combine the benefit of the mercury arc lamp for high precision DNA measurement and the high radiance of the laser for sensitive FITC analysis. The high precision in the DNA analysis with the mercury arc lamp is attributed to its strong output at 365 nm for fluorescence excitation of DAPI and to the fact that it readily provides uniform illumination in the sensing volume by the Köhler system. Highly specific and sensitive measurements can also be done with a conventional dual laser flow cytometer that provides ultraviolet and blue excitation light. In addition to the high cost of dual laser machines, another drawback of this system is that it appears to be relatively difficult to obtain a high precision in the analysis of nuclear DNA content compared with arc lamp-based flow cytometers. An alternative approach would be to use a single laser instrument, stain with propidium iodide instead of DAPI, excite fluorescence of propidium iodide and FITC at 488 nm, and compensate for effects of spectral overlap. However, this usually results in decreased sensitivity of FITC analysis at low signal levels.

The method used in this study gave reproducible results when applied to a series of paraffin-embedded lymphoma samples and provided significant clinical prognostic information about the correlation of survival time with the fraction of apoptotic cell nuclei, whereas no correlation of survival time was found with proliferative activity as determined by the fraction of S-phase cells (Castaños-Vélez et al, 1999). This indicates that, in these lesions, apoptosis was the stronger determinant of tumor growth. The developed assay could thus be used to further clarify the significance of the balance between cell proliferation and cell death in tumor growth and to elucidate the effect (apoptosis) of various treatment modalities.

Materials and Methods

Preparation and Fixation of Cell and Tissue Specimens

Cells from the myelomonocytic cell line U937 were centrifuged in a Ficoll-Paque density gradient (Pharmacia Biotech, Uppsala, Sweden). Aliquots of the enriched fraction of living cells (98% by Trypan blue exclusion) were cultured for 12 hours and then exposed to 4 ng/ml or 40 ng/ml of recombinant human TNF α for up to 24 hours. At different times, cells were washed in PBS and resuspended in fresh 4% paraformaldehyde (PFA) solution in PBS, pH 7.4. After overnight fixation at room temperature, part of the cell

preparation was pelleted, resuspended in 95% ethanol, and stored at -20°C . The other fixed cells were centrifuged, quickly resuspended in agar solution (1% in water), and allowed to solidify for 20 minutes at 4°C . Specimens of cells in coagulated agar were processed by routine embedding in paraffin.

The tonsil tissue preparations were from diagnostic biopsies of chronic tonsillitis, and the thymus was from a case of myasthenia gravis. The biopsy materials were cut into pieces of up to $2 \times 2 \times 2 \text{ mm}^3$ and fixed for approximately 16 hours in PFA solution, and one part of each sample was transferred to 95% ethanol. The other part was processed and embedded in paraffin as for the cell preparations.

Suspensions of rat thymocytes, which were triggered in vitro to undergo apoptosis and fixed in formaldehyde and ethanol, were kindly supplied by Dr. Boris Zhivotovsky (Division of Toxicology, Karolinska Institute, Stockholm, Sweden) and served as a control.

Archival samples of formalin-fixed and paraffin-embedded lymphoma tissues, obtained in SIV-infected cynomolgus monkeys as previously described (Castaños-Vélez et al, 1999), were also evaluated in the study and included specimens from 10 primary lymphomas (9 monkeys) and 10 secondary tumors from inoculated severe combined immunodeficiency mice. In 18 samples, nonnecrotic tumor regions with less than 30% nonneoplastic reactive cells were selected for FCM analysis, whereas in 2 specimens approximately 25% and 40% of the tissues consisted of necrotic regions, respectively.

Enucleation, TUNEL Reaction, and DNA Staining

Cell Nuclei from Paraffin-Embedded Specimens. The Hedley-method for DNA analysis of paraffin-embedded tissues (Hedley et al, 1983) was applied with some modifications. Sections of $90 \mu\text{m}$ thickness were cut, deparaffinized, rehydrated, and enucleated with subtilisin Carlsberg (Heiden et al, 1991). In the preparations of cytoplasm-free nuclei, the protease was inactivated with one drop of PFA solution for 10 minutes, followed by washing (300 g, 10 minutes) in 95% ethanol or Tris buffer (0.1 M Tris, 0.07 M NaCl, pH 7.5) and storage at 4°C after counting. Aggregation of cell nuclei was apparently less, if Tris buffer was used in this step instead of ethanol. Thereafter, TUNEL was performed using the "In situ cell death detection kit fluorescein" (Boehringer Mannheim, Roche Molecular Biochemicals, Mannheim, Germany) according to the manufacturer's instructions. Finally, $300 \mu\text{l}$ DAPI solution ($5 \mu\text{M}$ DAPI in 500 mM trisodium citrate) was added and the intensity of the TUNEL staining was checked in the fluorescence microscope. The specificity of the TUNEL reaction was examined by morphological criteria such as condensation of chromatin and nuclear fragmentation.

Whole Cells and Cell Nuclei from Nonembedded Specimens. Tissue biopsies and suspensions of cultured cells (U937) were fixed overnight with PFA, stored in 70% ethanol, and either processed as whole cells (U937) with TUNEL and DAPI staining as de-

scribed before or washed twice in distilled water for 20 minutes before enucleation with subtilisin Carlsberg (Castro et al, 1993) and further processing as already described.

Flow Cytometry

Optical System. The optical configuration of the flow system used is shown schematically in Figure 5. In the flow chamber, each cell crosses sequentially two spatially separated regions of fluorescence excitation. In those regions, the fluorescence emissions of DAPI and FITC are excited consecutively with ultraviolet light at 365 nm and blue light at 488 nm and recorded by photomultiplier tubes. The instrument base is a Partec Flow Cytometer PASII (Partec, Münster, Germany), which was upgraded to a low-budget, double-beam flow cytometer with an air-cooled 16 mW argon-ion laser (Model 161B; Spectra-Physics, Mountain View, California) and a custom-manufactured, triple-window dichroic mirror (Melles-Griot, Stockholm, Sweden). This mirror shows high rejection at 365 nm, 488 nm, and 546 nm and good transmission in the blue (400–480 nm), green (500–540 nm), and orange-red ($>560 \text{ nm}$) spectral ranges. Its spectral characteristics are important for an effective use of the excitation and emission light intensities available. The instrument shows high signal-to-noise ratios in both channels used. The detection threshold in the green analysis channel is 820 molecules of equivalent soluble fluorochromes (MESF) units of FITC as determined with the "Quantum Fluorescence Kits for MESF Units of FITC" (Sigma Chemical, St. Louis, Missouri). The optics provide a high specificity of spectral isolation of DAPI and FITC fluorescence without leakage of green DAPI emission light into the analysis channel for FITC

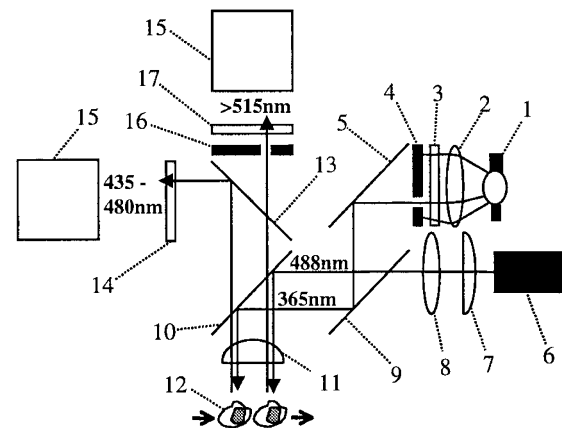


Figure 5.

Diagram of the flow cytometer optics. Mercury arc lamp HBO100 (1), collector (2), heat protection filters KG1 and BG38 and UG1 filter with peak transmission at 360 nm (3), slit radiant field stop (4), full mirror (5), 16 mW argon-ion laser (6), beam-shaping cylindrical (7) and spherical lenses (8), dichroic mirror with edge at 420 nm (9), dichroic triple mirror with high reflection at 365 nm, 488 nm, and 546 nm (10), 1.15 numerical aperture objective (11), flowing cell (12), dichroic long pass filter with edge at 500 nm (13), combined long pass filter with edge at 435 nm and short pass filter with edge at 480 nm (14), photomultiplier tubes (15), slit measuring field stop (16), and long pass barrier filter with edge at 515 nm (17).

detection (Fig. 6, a to c). Commercially available double-beam flow cytometers with sources of ultraviolet and blue excitation light can also be used.

Calculation of Cell-Fractions in S-Phase and Labeled by TUNEL. The negative control of the TUNEL reaction was used to define the decision boundary for counting of TUNEL-positive events with the analysis software of the PASII (Fig. 6d). Subregions for counting of TUNEL-positive and -negative sub-G1- and G1-events are indicated in Figure 2. CV values of G1 cells and fractions of S-phase cells were calculated with the MulticycleAV program (Phoenix Flow Systems, San Diego, California).

TUNEL-Reactivity in Tissue Sections

The TUNEL reaction was performed on deparaffinized tissue sections (5- μ m thick) using the "In situ cell death detection kit POD" (Boehringer Mannheim, Roche Molecular Biochemicals, Stockholm, Sweden) according to the manufacturer's instructions. At least one thousand cells per sample were scored in a microscope (BX-60; Olympus, Tokyo, Japan) equipped with a digital camera (DKC-5000; Sony, Tokyo, Japan).

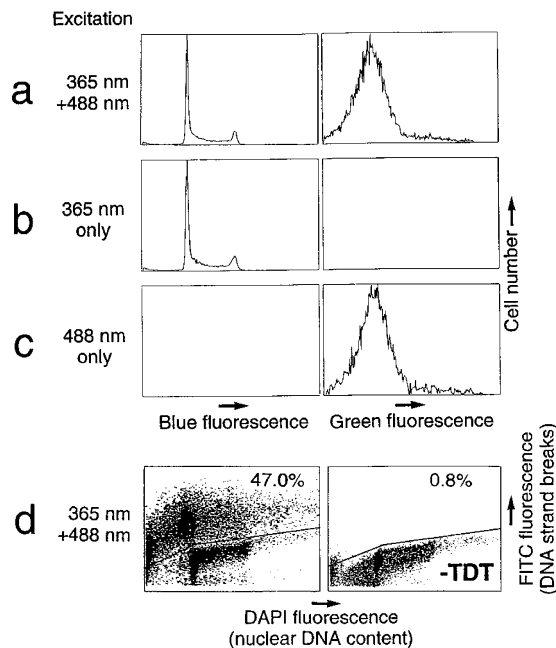


Figure 6.

Flow data on controls of spectral isolation of fluorochrome emission and specificity of TUNEL-labeling of U937 cells. Cells in spontaneous apoptosis (a to c) and after treatment (24 hours) with $\text{TNF}\alpha$ (d) were fixed (PFA), FITC-labeled by the TUNEL reaction, stained with DAPI, and analyzed as whole cells. In the TUNEL control (-TDT), the TDT-enzyme was omitted. The cells were analyzed by FCM at unchanged gain settings using single fluorescence excitation at 365 nm and 488 nm, respectively, and dual wavelength excitation. Spectral isolation of DAPI and FITC fluorescence was highly specific (a to c). The negative control was used to determine a decision boundary (*line*) for counting of TUNEL-positive cells. Fractions of events above the line are indicated.

Acknowledgements

We thank Prof. Bernhard Tribukait for providing the flow cytometer and other facilities.

References

- Baretton GB, Diebold J, Christoforis G, Vogt M, Müller C, Dopfer K, Schneiderbanger K, Schmidt M, and Löhrs U (1996). Apoptosis and immunohistochemical bcl-2 expression in colorectal adenomas and carcinomas. *Cancer* 77: 255-264.
- Barlogie B, Raber MN, Schumann J, Johnson TS, Drewinko B, Swartzendruber DE, Göhde W, Andreef M, and Freireich EJ (1983). Flow cytometry in clinical cancer research. *Cancer Res* 43:3982-3997.
- Castañón-Vélez E, Heiden T, Ekman M, Lawrence J, Biberfeld G, and Biberfeld P (1999). Proliferation and apoptosis-related gene expression in experimental AIDS-related simian lymphoma. *Blood* 93:1364-1371.
- Castro J, Heiden T, Wang N, and Tribukait B (1993). Preparation of cell nuclei from fresh tissues for high-quality DNA flow cytometry. *Cytometry* 14:793-804.
- Czader M, Mazur J, Pettersson M, Liliemark J, Strömberg M, Christensson B, Tribukait B, Auer G, Öst Å, and Porwit A (1996). Prognostic significance of proliferative and apoptotic fractions in low grade follicle center cell-derived non-Hodgkin's lymphomas. *Cancer* 77:1180-1188.
- Dowsett M, Detre S, Ormerod MG, Ellis PA, Mainwaring PN, Tittley JC, and Smith IE (1998). Analysis and sorting of apoptotic cells from fine-needle aspirates of excised human primary breast carcinomas. *Cytometry* 32:291-300.
- Dowsett M, Ellis PA, Saccani-Jotti G, Johnston SRD, Salter J, Anderson E, Nicholson R, and Howell A (1996). Tamoxifen and the pure antiestrogen ICI 162780 induce apoptosis in oestrogen receptor positive primary breast cancer in vivo. *Proc Am Assoc Cancer Res* 37:185.
- Ellis PA, Detre S, Burton SA, Salter J, Johnston SRD, Smith IE, and Dowsett M. (1996). Changes in proliferation, apoptosis, and bcl-2 in breast cancer specimens following neoadjuvant chemotherapy. *Breast Cancer Res Treat* 37:36.
- Ellis PA, Smith IE, Salter J, Detre S, O'Brien MER, Ramage F, and Dowsett M (1997). Preoperative chemotherapy induces apoptosis in early breast cancer. *Lancet* 349:849.
- Fisher DE (1994). Apoptosis in cancer therapy: Crossing the threshold. *Cell* 78:539-542.
- Gavrieli Y, Sherman Y, and Ben-Sasson (1992). Identification of programmed cell death in situ via specific labeling of nuclear DNA fragmentation. *J Cell Biol* 119:493-501.
- Gorczyca W, Gong J, Ardelit B, Traganos F, and Darzynkiewicz Z (1993). The cell cycle related differences in susceptibility of HL-60 cells to apoptosis induced by various antitumor agents. *Cancer Res* 53:3186-3192.
- Gorczyca W, Tuziak T, Kram A, Melamed MA, and Darzynkiewicz Z (1994). Detection of apoptosis-associated DNA strand breaks in fine-needle aspiration biopsies by in situ end labeling of fragmented DNA. *Cytometry* 15:169-175.
- Hedley DW, Friedlander ML, Taylor IW, Rugg CA, and Musgrove EA (1983). Method for analysis of cellular DNA content of paraffin-embedded pathological material using flow cytometry. *J Histochem Cytochem* 31:1333-1335.

Heiden T, Wang N, and Tribukait B (1991). An improved Hedley method for preparation of paraffin-embedded tissues for flow cytometric analysis of ploidy and S-phase. *Cytometry* 12:614–621.

Lipponen P, Aaltomaa S, Kosma VM, and Syrjänen K (1994). Apoptosis in breast cancer as related to histopathological characteristics and prognosis. *Eur J Can* 30A:2068–2073.

Listman JA, Wang Y, Castro JE, Rimm IJ, Finn PW, and Perkins DL (1998). Detection of rare apoptotic T cells in vivo. *Cytometry* 33:340–347.

Olano JP, Wolf D, Keherly M, and Gelman BB (1996). Quantifying apoptosis in banked human brains using flow cytometry. *J Neuropathol Exp Neurol* 55:1164–1172.

Samoszuk MK, Sallash G, Chen K, Carlton E, and Oldaker T (1996). Association between flow cytometric S-phase fraction and apoptotic rate in breast cancer. *Cytometry* 26:281–285.